Macromolecules

Article

pubs.acs.org/Macromolecules

When Ends Meet: Circular DNA Stretches Differently in Elongational Flows

Yanfei Li,[†] Kai-Wen Hsiao,[‡] Christopher A. Brockman,[‡] Daniel Y. Yates,[§] Rae M. Robertson-Anderson,[∥] Julia A. Kornfield,[⊥] Michael J. San Francisco,[§] Charles M. Schroeder,[‡] and Gregory B. McKenna*[,†]

[†]Department of Chemical Engineering, Texas Tech University, Lubbock, Texas 79409, United States

[‡]Department of Chemical & Biomolecular Engineering, University of Illinois at Urbana−Champaign, Urbana, Illinois 61801, United States

[§]Department of Biological Sciences, Texas Tech University, Lubbock, Texas 79409, United States

[∥]Department of Physics, University of San Diego, San Diego, California 92110, United States

[⊥]Division of Chemistry & Chemical Engineering, California Institute of Technology, Pasadena, California 91125, United States

ABSTRACT: Chain topology has a profound impact on the flow behavior of single macromolecules. For circular polymers, the absence of free ends results in a unique chain architecture compared to linear or branched chains, thereby generating distinct molecular dynamics. Here, we report the direct observation of circular DNA dynamics in transient and steady flows for molecular sizes spanning the range of 25.0−114.8 kilobase pairs (kbp). Our results show that the longest relaxation times of the rings follow a power-law scaling relation with molecular weight that differs from that of linear chains. Also, relative to their linear counterparts, circular DNA molecules show a shifted coil-to-stretch transition and less diverse "molecular individualism" behavior as evidenced by their conformational stretching pathways. These results show the impact of chain topology on dynamics and reveal commonalities in the steady state behavior of circular and linear DNA that extends beyond chain architecture.

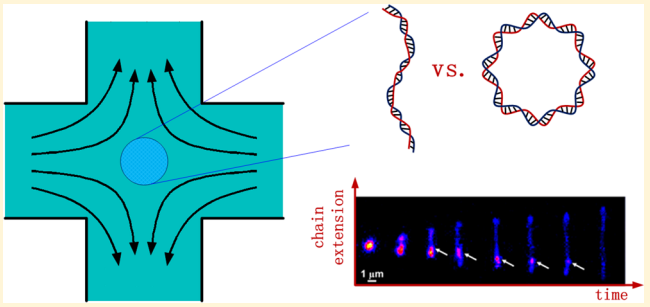

1. INTRODUCTION

Circular macromolecules play a key role in biology and biotechnology, including DNA replication and maintenance of circular genomes,[1] DNA looping,[2] plasmid-based DNA vaccines,[3] and biologically active macrocycles as drugs.[4] Circular macromolecules call into question our understanding of polymer dynamics because the absence of free ends alters flow behavior,[5,6] diffusion,[7,8] and ordering transitions[9] compared to linear macromolecules. For these reasons, achieving a clear understanding of circular polymer dynamics in nonequilibrium conditions has been a major task.[10,11] In this work, we observe the conformational and orientational dynamics of large circular DNA molecules in a planar extensional flow using single molecule techniques. Extensional flow consists of an axis of compression and an orthogonal axis of extension free of fluid rotation. For this reason, extensional flow is considered a "strong flow" capable of stretching polymers to high extension and is used in many processes such as flow-assisted DNA sequencing,[12] plasmid purification,[13] DNA electrophoresis,[14,15] and turbulent drag reduction.[16] It is known that long linear polymers undergo a coil-to-stretch transition (CST) in steady state extensional flows,[17,18] generally exhibiting "molecular individualism" during the transient stretching process:[18−21] using λ-phage DNA, Chu and co-workers[18,19] discovered that identical polymers pass through different transient conformations under identical flow conditions due to subtle differences in their initial shapes and a delicate balance between convection and diffusion.

By moving beyond linear polymers, we aim to improve our understanding of the role of molecular topology on the stretching dynamics of polymers with nonlinear topologies in flow. In particular, we performed single molecule experiments on large circular DNA polymers in order to provide quantitative comparisons of the conformational dynamics of monodisperse circular polymers to address key questions including the following: (1) Does circular DNA exhibit a CST, and if so, how does it compare to that of the linear chain of similar size? (2) How does molecular individualism in the transient response of circular macromolecules compare to the linear chain response? (3) What are the underlying commonalities and differences among different polymer topologies, e.g., scaling of longest relaxation time and conformational stretching pathways? Importantly, answers to these questions will help reveal the influence of molecular architecture on the dynamics of macromolecules.

Received: June 23, 2015
Revised: July 25, 2015
Published: August 7, 2015

ACS Publications © 2015 American Chemical Society

DOI: 10.1021/acs.macromol.5b01374
Macromolecules 2015, 48, 5997−6001

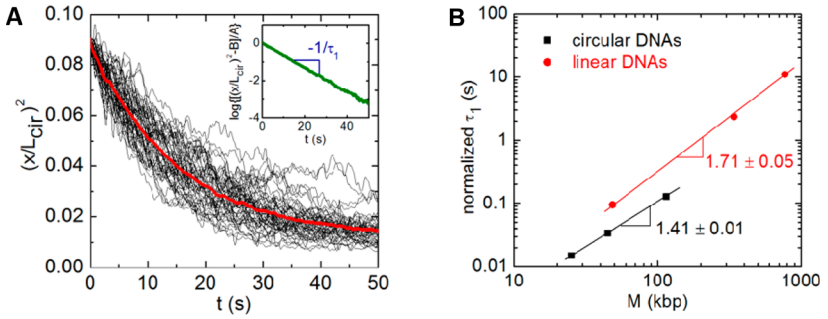

Figure 1. (A) Single molecule relaxation trajectories of 114.8 kbp circular DNA (solvent viscosity η_s = 123.6 mPa·s). The red solid line indicates the average over 52 molecules. The inset shows the semilogarithmic plot of $\log\{[\langle x(t)\rangle/L_{cir})2 - B]/A\}$ as a function of time, where the slope is $-\tau_1^{-1}$. (B) Relaxation times for linear and circular DNA as a function of molecular weight M. Data for the linear DNA (~339.5 kbp and ~800 kbp) is from literature.[18,30,31] For comparison, all relaxation times are normalized by solvent viscosity η_s to the case where η_s = 1 mPa·s. The error bars are smaller than the sizes of the symbols.

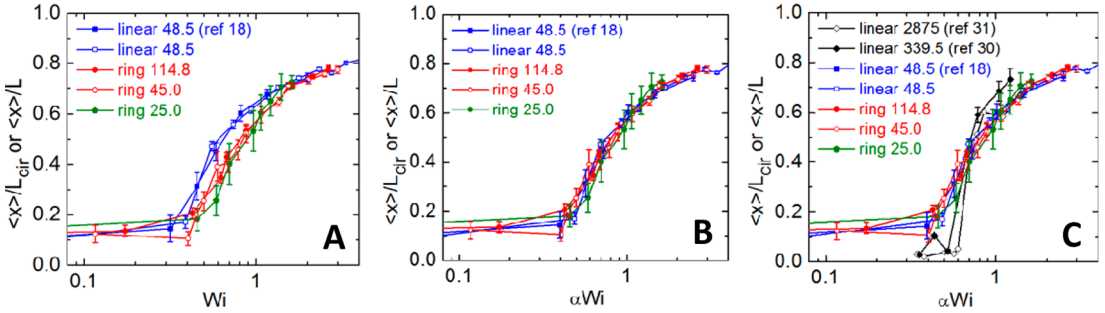

Figure 2. (A) Steady state fractional extension of linear and circular DNA in planar extensional flow as a function of Wi for 25.0 kbp ring, 45.0 kbp ring, 114.8 kbp ring, and 48.5 kbp linear DNA. For 48.5 kbp linear DNA, one set of data is obtained from the present study and the other from ref 18. (B) Comparison of data of Figure 2A obtained upon shifting the data along the Wi axis (shift factor α = 1.0 for ring DNA and α = 1.25 for linear 48.5 kbp DNA). (C) Comparison of data to two much longer linear DNA molecules (339.5 kbp and 2875 kbp, from refs 30 and 31). The data of all three linear DNAs are shifted along the Wi axis (shift factor α = 1.0 for ring DNA and α = 1.25 for all linear DNA).

2. EXPERIMENTAL SECTION

In this work, we prepared circular DNA polymers using bacterial cell hosts and standard cloning methods for fosmids and bacterial artificial chromosomes (BACs). DNA was extracted from *Escherichia coli* cells by following the procedures of Laib et al.[22] In particular, TransforMax EPI300 Electrocompetent *E. coli* was used as the host to produce 25.0 kbp fosmid (Fos25, contour length of linear analogue L = 8.5 μm). L is the contour length of a linear or circular DNA. However, due to the cyclic topology of the circular DNA, its maximum projection in the direction of extension is halved, i.e., $L_{cir} = L/2$. 45 kbp fosmid (Fos45, L = 15.3 μm) and 114.8 kbp BAC (K16, L = 39.0 μm). For comparison, the crystallographic contour length of λ-phage DNA (48.5 kbp) is L = 16.5 μm. The molecules were fluorescently labeled with an intercalating dye (YOYO-1, dye: base pair =1:4), which increases the contour length by a factor of 1.3, consistent with prior reports for linear DNA chains.[23] To fluorescently label the DNA molecules, the DNA samples were mixed with YOYO-1 (Invitrogen™) at a dye-to-base-pair ratio of 1:4, in an aqueous buffer containing 30 mM Tris (pH = 8), 5 mM NaCl, 2 mM EDTA. The mixture was kept in the dark and gently swirled at room temperature for 1 h.

Following sample preparation, a mixture containing mainly relaxed circular DNA with a small amount of linear and supercoiled DNA was injected into a microfluidic flow cell[24] and only relaxed circular molecules were analyzed based on visual inspection of the molecular extension of highly stretched circular DNA in flow. We directly visualize circular polymer relaxation and stretching dynamics using single molecule fluorescence microscopy (SMFM). All experiments were carried out at 23 °C. The imaging buffer contains 30 mM Tris (pH = 8), 5 mM NaCl, 2 mM EDTA, 5 mg/mL glucose, 4% β-mercaptoethanol, glucose oxidase (0.05 mg/mL), and catalase (0.01 mg/mL). Sucrose is added to adjust the viscosity of the solution. An automated feedback-controlled microfluidic device known as a "microfluidic trap"[24] was used to study chain dynamics and molecular individualism. Specifically, DNA molecules were trapped near the stagnation point of a planar extensional flow field for hundreds of seconds to enable the imaging of the single chain dynamics during multiple cycles of extension and relaxation. Imaging and detection were done by an inverted epifluorescence microscope coupled to an Andor CCD camera. Molecules were illuminated by a blue laser (400–500 nm). Light was collected by a 1.45NA, 100× oil immersion objective. Pixels were binned 1 × 1, giving 1 μm × 1 μm pixels. Images were sampled at an interval of 0.0315 s.

3. RESULTS AND DISCUSSION

Longest Polymer Relaxation Time. DNA molecules were stretched in extensional flow to ~70% of the maximum extension (~$0.7L_{cir} = 0.7L/2$), followed by direct observation of chain relaxation upon flow cessation. The longest relaxation time τ_1 was evaluated using a single exponential fit to the relaxation of the average fractional extension with time after cessation of flow such that $(\langle x(t)\rangle/L_{cir})^2 = A\exp(-t/\tau_1) + B$, where $x(t)$ is the instantaneous maximum projected polymer extension and the fit is performed over the linear force region where $\langle x(t)\rangle/L_{cir} < 0.3$, and A and B are fitting constants (Figure 1A).

It is of particular interest to understand how τ_1 scales with molecular weight M. Zimm theory[25] predicts a relaxation time scaling as $\tau_1 \sim M^{3\nu}$ and a diffusion coefficient that scales as $D \sim M^{-\nu}$, where the exponent ν = 0.5 for a theta solvent and $\nu \approx 0.6$ for a good solvent. Renormalization group (RG) theory[26] that accounts for intrachain excluded volume (EV) interactions predicts the same power-law exponent ν = 0.588 for linear and

DOI: 10.1021/acs.macromol.5b01374
Macromolecules 2015, 48, 5997–6001

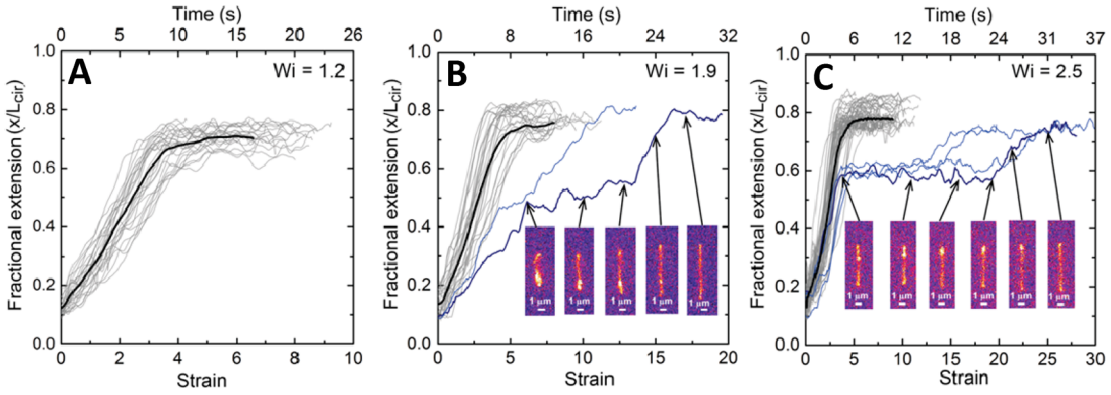

Figure 3. Transient stretching (x/L_{cir}) trajectories as a function of time t and strain ($\varepsilon = \dot{\varepsilon}t$) for the Fos45 circular polymer (τ_1 = 3 s) at three different Wi = 1.2, 1.9 and 2.5, in (A), (B), and (C), respectively. N is the number of trajectories. The black thick curve in each figure represents the ensemble average ($\langle x \rangle/L_{cir}$) of all individual trajectories. The "knot-formation" trajectories are colored in navy blue, and those stretch continuously are in gray color. To demonstrate the formation and disappearance of the transient knot, snapshots (corresponding to the thick navy blue curve) of the circular Fos45 molecules were taken at different stages and shown in Figure 3, parts B and C.

circular polymers. Within the range of M of interest here (25.0 to 114.8 kbp), circular polymers relax a factor of ~2.0−3.1 times faster than linear chains of the same M, and both circular and linear DNAs exhibit power-law behaviors (see Figure 1B, where τ_1 values are normalized to solvent viscosity η_s = 1 mPa·s). Interestingly, circular DNA shows a weaker dependence on M, in contrast with RG theory[26] and with diffusion studies[7] that found approximately the same power as a function of M (3ν = 1.76) for both circular and linear DNAs. The scaling exponent observed here for circular DNA is close to values (3ν = 1.4−1.6) reported for synthetic low molecular weight flexible ring polymers in good solvents.[27,28] The scaling exponent of the linear DNAs (3ν = 1.71) is close to that predicted by the Zimm model with EV (3ν = 1.76), whereas the smaller exponent (3ν = 1.41) for the ring molecules is close to the case of negligible EV effects (3ν = 1.5). A possible explanation is that for circular and linear DNAs of the same M, circular DNA is effectively 50% smaller in contour length. Moreover, Figure 1B compares data for relatively low M circular DNA to higher M linear DNA. Because of the smaller molecular weight for circular DNA, EV is expected to be less important, which would in turn decrease the scaling exponent of τ_1 as a function of M.[29]

Steady State Polymer Extension. Among nonequilibrium properties, one of particular importance is the existence of a coil-to-stretch transition (CST), which has been observed for linear polymers in extensional flows.[17−19] In Figure 2A, the steady state extension of circular DNA is plotted as a function of Weissenberg number Wi = $\tau_1\dot{\varepsilon}$, where $\dot{\varepsilon}$ is the fluid strain rate. The data clearly show a CST for circular DNA, and the shapes of the curves are similar to that of linear λ-DNA. Relative to linear DNA, the onset of stretching for circular DNA molecules occurs at a slightly larger critical $\mathrm{Wi}_{c,ring}$ = 0.40 (cf., $\mathrm{Wi}_{c,linear}$ = 0.32), meaning circular DNA is less prone to stretch under the same normalized flow strength Wi.

The similar shapes of elongation curves in Figure 2A motivated us to rescale the dimensionless flow strength Wi for the 48.5 kbp linear DNA by a factor of $\alpha = \mathrm{Wi}_{c,ring}/\mathrm{Wi}_{c,linear}$ = 0.4/0.32 = 1.25, which nicely superimposes all curves (Figure 2B). We hypothesize that the shift factor α = 1.25 arises due to intramolecular hydrodynamic interactions (HI). In the coiled state, intramolecular HI is more important for circular DNA compared to linear DNA due to its more compact structure, and therefore, the onset of stretching is delayed and shifted to a slightly higher Wi. Upon stretching from the coiled state, Brownian dynamics simulations by Schroeder et al.[30] suggest that HI tends to increase the slope of the CST and the magnitude of the extension in the stretched state. It is interesting that the slope of the CST and the magnitude of the extension match for the linear and circular DNA in this size range. Another possible explanation for the shift factor (α = 1.25), is that it may simply require a stronger flow to stretch a circular macromolecule, due to the fact that a circular polymer effectively has twice the tension (approximately) compared to a linear chain. However, both of the explanations above are qualitative, and ideally, simulation techniques need to be employed to reveal the mechanisms in a quantitative way.

Moving beyond the coiled state of the polymer chain, it has been shown that HI does not substantially affect λ-DNA in the extended state.[30] In this sense, the superimposability of the data in Figure 2 indicates that HI is relatively unimportant for circular DNA in the stretched state. This confirms the notion[30,32−34] that DNA molecules with molecular weight M in the range ~10−100 kbp are affected by HI near equilibrium, yet relatively free of these effects once they are stretched. The minor role of HI in the stretched state of circular and linear DNA in this work is further illustrated by comparison with two much larger linear DNAs, which exhibit much sharper CST transitions and the higher fractional extensions at Wi > 1.0 (Figure 2C, with data for all three linear DNAs being shifted by α = 1.25). From a fundamental perspective, the superimposability suggests the existence of an underlying commonality governing chain dynamics that describes both circular and linear topologies in determining the steady state flow behavior. Further, the shapes of the curves are independent of molecular size up to 115 kbp for circular DNA, which suggests that this set of data can serve as a "reference state" for polymers with a minor role of HI during the stretching process. For circular DNA molecular larger than M ~ 600 kbp, we hypothesize that intramolecular HI will influence chain dynamics in the coil-to-stretch transition. Finally, for the data shown in Figure 2, one can combine the ratio of longest polymer relaxation times for linear to circular DNA ($\tau_{1,linear}/\tau_{1,ring}$ = 2.5) with the ratio of critical Wi (α = 1.25), thereby yielding the ratio of critical extension rates for circular and linear DNA is $\dot{\varepsilon}_{c,ring}/\dot{\varepsilon}_{c,linear}$ = 3.1. This value is slightly smaller but in reasonable accord with

DOI: 10.1021/acs.macromol.5b01374
Macromolecules 2015, 48, 5997−6001

the value of 4.1 obtained by Cifre et al. in Brownian dynamics simulations[35] of flexible polymers in uniaxial extensional flows.

Molecular Individualism. We further characterized chain conformation during the transient stretching process by observing the extension of a single molecule during repeated stretching/relaxing events until irreversible photocleavage. To ensure a completely random initial state for each transient, we allowed the molecule to relax to an equilibrium configuration (without illumination) by waiting ~10 τ_1 between transient extension experiments. In order to characterize molecular individualism, we studied the Fos45 circular DNA molecules, which have a similar contour length to linear λ-DNA.[18,19] We conducted a series of transient stretching experiments at three different Wi on Fos45. For all values of Wi under investigation, molecular individualism occurs for the circular Fos45 (Figure 3), but the spread and diversity in the unraveling dynamics due to molecular individualism is not as great as previously observed for 48.5 kbp linear DNA.[18,19] In prior work, Perkins et al.[18] found that λ-DNA adopts four different molecular conformations while stretching in planar extensional flow: dumbbell, half-dumbbell, kinked, and folded states. In the context of stretching, folded conformations generally exhibit the slowest unraveling dynamics in flow. In the present study, we see only two types of trajectories for the circular Fos45 DNA: continuous elongation and interrupted elongation. This reduced individualism of circular DNA relative to linear DNA is consistent with the anticipation that circular DNA molecules have fewer degrees of freedom due to their chain connectivity.

The vast majority of molecular trajectories extend in a relatively smooth fashion, as in Figure 3A. During a smooth unraveling event, a molecule extends continuously and adopts a dumbbell configuration, which has been previously observed for linear λ-DNA (Figure 4A). On the other hand, interrupted elongation appears to be related to a few cases where a transient "knot" is observed during the stretching process (Figure 4B). In the case of a transient knot, the elongation tends to pause at an intermediate state until the knot is resolved (Figure 3, parts B and C). Upon release of the knot, the chain extension approaches the steady state value. The formation of knots depends on the flow strength Wi with several interesting features. First, the transient knot forms more frequently at higher Wi (no knots were observed at Wi = 1.2 (N = 30), 2 knots were observed at Wi = 1.9 (N = 30), and 4 knots were observed at Wi = 2.5 (N = 60)). These data suggest that molecular individualism becomes richer and more diverse at higher Wi, which qualitatively agrees with the experiments on linear λ-DNA.[20] Second, knots at the higher flow strength (Wi = 2.5) appear earlier and persist for longer durations compared to knots at lower flow strengths (Wi = 1.9). Polymer conformations that give rise to transient knots essentially trap the molecule in a metastable state that requires time to unravel. We hypothesize that the rate of escape from the knotted state slows down substantially as convection begins to outweigh Brownian diffusion at higher Wi or Péclet numbers (Pe).

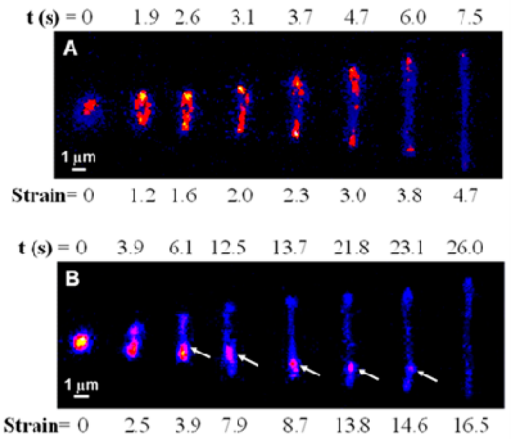

Figure 4. Time lapse images of single circular DNA polymers unraveling in flow. Images show two transient configurations for the circular Fos45 DNA including (A) uniform stretching at Wi = 1.9, and (B) the formation and unraveling of a transient knot at Wi = 1.9. The arrows in part B indicate the location of the knot. Image contrast and brightness has been enhanced for display purposes.

4. CONCLUSION

On the basis of our observations, there appear to be distinct commonalities and differences between linear and circular polymers in flow. Both linear and circular DNA polymers follow a power-law scaling of the longest relaxation time τ_1 as a function of molecular weight M. However, circular DNA relaxes faster and shows a lower scaling exponent 3ν. Both linear and circular macromolecules exhibit a coil-to-stretch transition in extensional flow; however, circular molecules begin to stretch at a higher Wi, and superimposability between linear λ-DNA and all circular DNAs is observed with a horizontal shift factor of α = 1.25. Moreover, circular DNA shows less diverse molecular individualism in conformational stretching pathways during transient extension, presumably due to the low diversity of initial states available to the circular molecules.

Given these observations, what are the implications for the role of polymer chain topology on dynamics and physics? Despite extensive studies on linear DNA,[30,32,34] a wide array of fundamental questions remain unresolved, including systematic methods for modeling and choosing parameters for coarse-grained simulations[36−38] (i.e., persistence length, degree of coarse graining) and investigating the roles of intramolecular HI,[32,33] EV,[29] self-entanglements, and internal viscosity[37] on polymer dynamics in dilute solutions. Our experimental data will provide a solid basis to examine these questions from a theoretical perspective, i.e., by extending our current understanding of the aforementioned effects for linear DNA to circular polymers. In a broader sense, the structure−property relationships established here using different molecular architectures and molecular weights provide guidance in the design of macromolecules to tune their rheological properties.[15,39] As an example, the chain extension data presented here would serve as a reference for modeling and designing the extensional viscosity of polymer solutions. Furthermore, the optimization of many biological applications requires an understanding of the elongational properties of DNAs.[2,3,12−15,40,41] Hence, from a biological perspective, this work may also provide a first level view of the issues related to the circularization and replication of early DNA molecules that occurred before the origin of prokaryotic and eukaryotic cells.[42] Natural selection for circular DNA molecules, particularly plasmids that can be mobilized from cell to cell, may be a function of the physical properties demonstrated here.[43]

AUTHOR INFORMATION

Corresponding Author

*E-mail: greg.mckenna@ttu.edu (G.B.M.).

DOI: 10.1021/acs.macromol.5b01374
Macromolecules 2015, 48, 5997−6001

Notes

The authors declare no competing financial interest.

■ ACKNOWLEDGMENTS

The work at TTU Chemical Engineering was supported by the John R. Bradford Endowment and the Paul Whitfield Horn Professorship. The work at UIUC was funded by a Dow Graduate Fellowship for K.-W.H. and C.A.B., and the David and Lucile Packard Foundation, NSF CAREER Award CBET-1254340, and the Camille and Henry Dreyfus Foundation for C.M.S. R.M.R.-A. was funded by the AFOSR Young Investigator Program, Grant No. FA95550-12-1-0315.

■ REFERENCES

(1) Blattner, F. R.; Plunkett, G., 3rd; Bloch, C. A.; Perna, N. T.; Burland, V.; Riley, M.; Collado-Vides, J.; Glasner, J. D.; Rode, C. K.; Mayhew, G. F.; Gregor, J.; Davis, N. W.; Kirkpatrick, H. A.; Goeden, M. A.; Rose, D. J.; Mau, B.; Shao, Y. *Science* **1997**, *277*, 1453−1462.
(2) Rao, S. S.; Huntley, M. H.; Durand, N. C.; Stamenova, E. K.; Bochkov, I. D.; Robinson, J. T.; Sanborn, A. L.; Machol, I.; Omer, A. D.; Lander, E. S.; Aiden, E. L. *Cell* **2014**, *159*, 1665−1680.
(3) Fynan, E. F.; Webster, R. G.; Fuller, D. H.; Haynes, J. R.; Santoro, J. C.; Robinson, H. L. *Proc. Natl. Acad. Sci. U. S. A.* **1993**, *90*, 11478−11482.
(4) Mallinson, J.; Collins, I. *Future Med. Chem.* **2012**, *4*, 1409−1438.
(5) Kapnistos, M.; Lang, M.; Vlassopoulos, D.; Pyckhout-Hintzen, W.; Richter, D.; Cho, D.; Chang, T.; Rubinstein, M. *Nat. Mater.* **2008**, *7*, 997−1002.
(6) Halverson, J. D.; Lee, W. B.; Grest, G. S.; Grosberg, A. Y.; Kremer, K. *J. Chem. Phys.* **2011**, *134*, 204905.
(7) Robertson, R. M.; Laib, S.; Smith, D. E. *Proc. Natl. Acad. Sci. U. S. A.* **2006**, *103*, 7310−7314.
(8) Robertson, R. M.; Smith, D. E. *Proc. Natl. Acad. Sci. U. S. A.* **2007**, *104*, 4824−4827.
(9) Wang, J.; Li, Z.; Pérez, R. A.; Müller, A. J.; Zhang, B.; Grayson, S. M.; Hu, W. *Polymer* **2015**, *63*, 34−40.
(10) McLeish, T. C. B. *Science* **2002**, *297*, 2005−2006.
(11) Bielawski, C. W.; Benitez, D.; Grubbs, R. H. *Science* **2002**, *297*, 2041−2044.
(12) Dylla-Spears, R.; Townsend, J. E.; Jen-Jacobson, L.; Sohn, L. L.; Muller, S. J. *Lab Chip* **2010**, *10*, 1543−1549.
(13) Han, J.; Craighead, H. G. *Science* **2000**, *288*, 1026−1029.
(14) Chen, Z.; Dorfman, K. D. *Electrophoresis* **2014**, *35*, 654−661.
(15) Saha, S.; Heuer, D. M.; Archer, L. A. *Electrophoresis* **2006**, *27*, 3181−3194.
(16) Lumley, J. L. *Annu. Rev. Fluid Mech.* **1969**, *1*, 367−384.
(17) de Gennes, P. G. *J. Chem. Phys.* **1974**, *60*, 5030−5042.
(18) Perkins, T. T.; Smith, D. E.; Chu, S. *Science* **1997**, *276*, 2016−2021.
(19) Smith, D. E.; Chu, S. *Science* **1998**, *281*, 1335−1340.
(20) Larson, R. G.; Hu, H.; Smith, D. E.; Chu, S. J. *J. Rheol.* **1999**, *43*, 267−304.
(21) de Gennes, P. G. *Science* **1997**, *276*, 1999−2000.
(22) Laib, S.; Robertson, R. M.; Smith, D. E. *Macromolecules* **2006**, *39*, 4115−4119.
(23) Kundukad, B.; Yan, J.; Doyle, P. S. *Soft Matter* **2014**, *10*, 9721−9728.
(24) Tanyeri, M.; Schroeder, C. M. *Nano Lett.* **2013**, *13*, 2357−2364.
(25) Zimm, B. H. *J. Chem. Phys.* **1956**, *24*, 269−278.
(26) Schaub, B.; Creamer, D. B. *Phys. Lett. A* **1987**, *121*, 435−442.
(27) Duval, M.; Lutz, P.; Strazielle, C. *Makromol. Chem., Rapid Commun.* **1985**, *6*, 71−76.
(28) Hodgson, D. F.; Amis, E. J. *J. Chem. Phys.* **1991**, *95*, 7653−7663.
(29) Sunthar, P.; Prakash, J. R. *Macromolecules* **2005**, *38*, 617−640.
(30) Schroeder, C. M.; Shaqfeh, E. S. G.; Chu, S. *Macromolecules* **2004**, *37*, 9242−9256.
(31) Schroeder, C. M.; Babcock, H. P.; Shaqfeh, E. S. G.; Chu, S. *Science* **2003**, *301*, 1515−1519.
(32) Jendrejack, R. M.; de Pablo, J. J.; Graham, M. D. *J. Chem. Phys.* **2002**, *116*, 7752−7759.
(33) Hsieh, C.-C.; Li, L.; Larson, R. G. *J. Non-Newtonian Fluid Mech.* **2003**, *113*, 147−191.
(34) Tree, D. R.; Muralidhar, A.; Doyle, P. S.; Dorfman, K. D. *Macromolecules* **2013**, *46*, 8369−8382.
(35) Hernández Cifre, J. G.; Pamies, R.; López Martínez, M. C.; García de la Torre, J. *Polymer* **2005**, *46*, 267−274.
(36) Underhill, P. T.; Doyle, P. S. *J. Non-Newtonian Fluid Mech.* **2004**, *122*, 3−31.
(37) Larson, R. G. *J. Rheol.* **2005**, *49*, 1−70.
(38) Somasi, M.; Khomami, B.; Woo, N. J.; Hur, J. S.; Shaqfeh, E. S. G. *J. Non-Newtonian Fluid Mech.* **2002**, *108*, 227−255.
(39) Ahirwal, D.; Filipe, S.; Neuhaus, I.; Busch, M.; Schlatter, G.; Wilhelm, M. *J. Rheol.* **2014**, *58*, 635−658.
(40) Ralston, E. J.; Schumaker, V. N. *Biophys. Chem.* **1979**, *9*, 375−381.
(41) Schlagberger, X.; Netz, R. R. *Macromolecules* **2008**, *41*, 1861−1871.
(42) Sagan, L. *J. Theor. Biol.* **1967**, *14*, 225−274.
(43) Forterre, P.; Filée, J.; Myllykallio, H. In *The Genetic Code and the Origin of Life*; de Pouplana, L. R., Ed.; Springer US: New York, 2004; Chapter 10, p 145.

DOI: 10.1021/acs.macromol.5b01374
Macromolecules 2015, 48, 5997−6001